JACS
JOURNAL OF THE AMERICAN CHEMICAL SOCIETY
Article
pubs.acs.org/JACS

Gas-Phase Azide Functionalization of Carbon

Eric D. Stenehjem, Vadim R. Ziatdinov, T. Daniel P. Stack, and Christopher E. D. Chidsey*

Department of Chemistry, Stanford University, Stanford, California 94305, United States

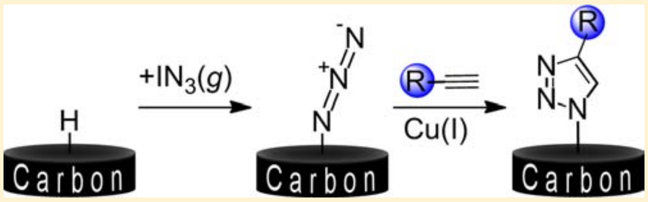

ABSTRACT: Tailoring the surface and interfacial properties of inexpensive and abundant carbon materials plays an increasingly important role for innovative applications including those in electrocatalysis, energy storage, gas separations, and composite materials. Described here is the novel preparation and subsequent use of gaseous iodine azide for the azide modification of carbon surfaces. In-line generation of gaseous iodine azide from iodine monochloride vapor and solid sodium azide is safe and convenient. Immediate treatment of carbon surfaces with this gaseous stream of iodine azide provides a highly reproducible, selective, and scalable azide functionalization that minimizes waste and reduces deleterious side reactions. Among the possible uses of azide-modified surfaces, they serve as versatile substrates for the attachment of additional functionality by coupling with terminal alkynes under the mild copper-catalyzed azide−alkyne cycloaddition (CuAAC) "click" reaction. For instance, coupling ethynylferrocene to azide-modified glassy carbon surfaces achieves ferrocene coverage up to 8×10^{13} molecules/cm^2 by voltammetric and XPS analyses. The 1,2,3-triazole linker formed during the CuAAC reaction is robust and hydrolytically stable in both aqueous 1 M $HClO_4$ and 1 M NaOH for at least 12 h at 100 °C.

INTRODUCTION

Carbon materials have found prominent use across a variety of applications including those in electrocatalysis, energy storage, gas separations, and composite materials. This extensive use results from not only the abundance and low-cost of carbon but also its desirable physical and chemical properties, such as high electrical and thermal conductivity, chemical stability, and range of structural forms (felts, fibers, foams, glasses, and powders). Furthermore, surface modification of carbon materials[1,2] allows for the introduction of additional functionality to tailor its surface and interfacial properties for the desired application. Surface modification strategies for the creation of these functional materials should ideally (1) have a robust linker between the introduced functionality and the surface, best provided by hydrolytically stable covalent bond formation[3,4] and (2) undergo selective transformations to create chemically well-defined surfaces, thus allowing for the rational design of materials.

A commonly used carbon surface functionalization methodology involves coupling with aryl radicals, which are formed in solution by the reduction of aryl diazonium salts, resulting in a robust and hydrolytically stable C−C bond to the surface.[5,6] However, the promiscuous reactivity of this aryl radical intermediate commonly leads to the formation of ill-defined multilayer structures up to 15 nm thick.[7] In select cases a monolayer has been achieved by degradation of the multilayer structure above,[8] use of steric blocking groups,[9,10] and localized electrogeneration of the diazonium.[11] Other methods for robust surface functionalization include radical coupling of amines,[12] coupling of alkynes at high temperatures,[13] and photochemical coupling with alkenes.[14,15] These relatively nonselective methods, while producing robust C−C or C−N bonds, are limited in scope to molecules tolerant to the harsh coupling conditions.

Another surface functionalization strategy is the introduction of a surface group onto which additional functionality can be coupled in subsequent chemical steps. Surface azides provide such a functional group that couples with terminal alkynes via a copper-catalyzed azide−alkyne cycloaddition (CuAAC) reaction[16,17] through formation of a 1,2,3-triazole linker, a "click" reaction.[18] The mild conditions of the CuAAC reaction tolerate many functional groups, including those in protein and nucleic acids, allowing a wide range of species to be coupled to azide-modified surfaces through attachment of a terminal alkyne group.[19,20] This strategy has been applied to carbon materials by using iodine azide (IN_3) solutions to produce azide-modified surfaces.[21,22]

Presented here is an alternative, simple, scalable, and chemically specific method for the highly reproducible azide functionalization of glassy carbon surfaces using IN_3 in the gas-phase. The procedure allows for $IN_3(g)$ to be prepared in-line safely and directly from commercially available chemicals along with minimizing waste and providing greater control of the reaction environment to reduce deleterious side reactions compared to solution iodine azide functionalization methodologies. Glassy carbon was chosen as a representative carbon material because of its favorable properties for electrochemical and surface analyses. These azide-modified surfaces can be coupled with terminal alkynes to form robust triazole linkers to the surface that are hydrolytically stable at elevated temperatures in both highly acidic and basic aqueous solutions.

Received: October 22, 2012
Published: January 9, 2013

dx.doi.org/10.1021/ja310410d | *J. Am. Chem. Soc.* 2013, 135, 1110−1116

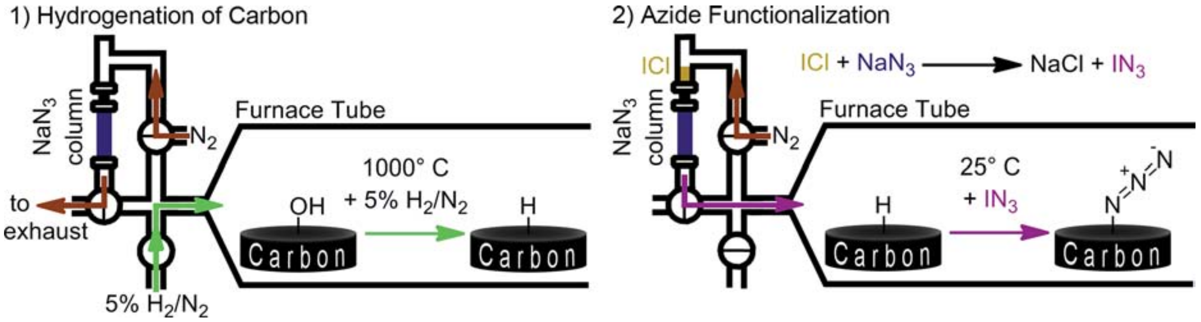

Figure 1. Gas-phase azide functionalization of carbon occurs in a two-step procedure: (1) Hydrogenation of carbon surfaces under forming gas. (2) Azide functionalization using $IN_3(g)$.

■ RESULTS

Gas-Phase Procedure for Azide Functionalization. As illustrated in Figure 1, polished glassy carbon disks were first hydrogenated under forming gas (5% H_2/N_2) at 1000 °C. After 90 min, the furnace was cooled to room temperature. ICl(l) was dispensed onto a bed of glass wool in the upper chamber of a flow reactor and its vapors were carried by $N_2(g)$ through a column of $NaN_3(s)$ dispersed on silica to form $IN_3(g)$ in the effluent gas stream. $IN_3(g)$ was identified by characteristic IR (2055 and 2065 cm^{-1})[23] and UV/vis (320[24] and 243 nm) absorbances along with $I_2(g)$ (530 nm);[25] no other species in appreciable quantities were detected (Figures 2 and 3).[26] This gas steam containing $IN_3(g)$ was passed over the hydrogenated carbon surfaces in the dark. The furnace tube was then purged with $N_2(g)$ before the glassy carbon was removed for analysis or further surface modification.

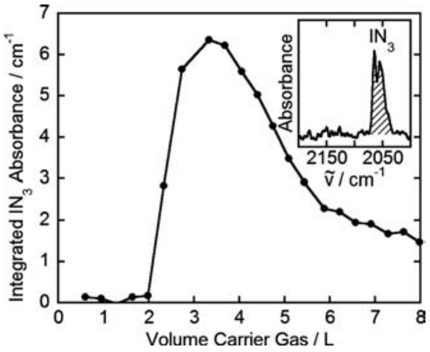

Figure 2. Integrated $IN_3(g)$ absorbance of the effluent gas stream through a 10 cm path length. Insert shows 2055 and 2065 cm^{-1} IR absorption peaks characteristic of $IN_3(g)$ (shaded).

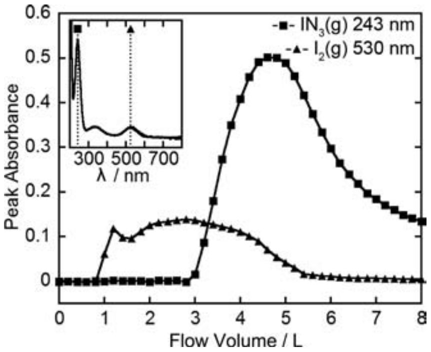

Figure 3. UV/vis absorbance of the effluent gas stream through a 10 cm path length. Insert shows UV/vis spectrum at maximum $IN_3(g)$ absorbance.

Treatment of hydrogenated carbon with this gas stream results in the addition of nitrogen and iodine to the surface as shown by X-ray photoelectron spectroscopy (XPS) (Figure 4).

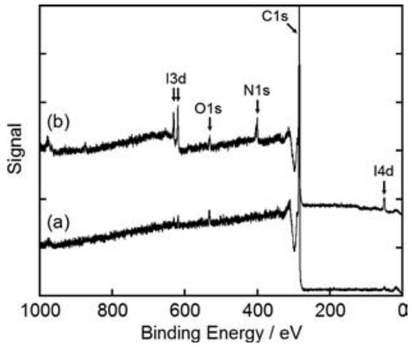

Figure 4. XPS spectra of (a) hydrogenated and (b) gas-phase azide-modified glassy carbon.

Atomic concentrations obtained from these spectra were highly reproducible between preparation cycles (Table 1, entry 2). Two peaks with binding energies of 404 and 400 eV appear in the XPS N 1s region (Figure 5a). An azide group is expected to have two peaks with a ratio of 1:2 in this region; the central nitrogen exhibits a higher binding energy than the two outer nitrogens.[27] A two-component fit suffices to model these peaks, one for the distinct higher binding energy central azide nitrogen and the other representative of the outer two nitrogens of the azide plus other nitrogen species. The higher energy component was fixed at 403.9 eV with a width of 2.0 eV, while the other component was left unconstrained. Fitting the N 1s region (Figure 5a) for gas-phase azide-modified surfaces results in a ratio of 1:2.0, consistent with azides as the sole nitrogen species (Table 1, entry 2).

The IN_3 gas-phase procedure was varied to determine factors critical for reproducible preparations. Omission of either ICl(l) or $NaN_3(s)$ resulted in no formation of $IN_3(g)$ and no nitrogen addition to the carbon surface (Table 1, entries 3 and 4). In the omission of $NaN_3(s)$, ICl(g) (467 nm)[28] was observed by UV/vis in the effluent gas stream, which correlated to the addition of iodine and chlorine to the carbon surfaces (Table 1, entry 4). The absence of a peak at 467 nm in the effluent gas stream during the standard gas-phase procedure suggests complete consumption of ICl. Minimization of water, including the use of dried N_2 carrier gas, is critical for the reproducibility of this gas-phase procedure. Hydrated $NaN_3(s)$ dispersed on silica (~5%

Table 1. XPS Surface Atomic Concentrations of Carbon Samples after Indicated Procedure

entry	procedure	C at. %[a]	N at. %[a]	Azide at. %[a]	O at. %[a]	I at. %[a]	Cl at. %[a]
1	hydrogenation	98(2)	0.0(3)	0.0(1)	2(1)	0.03(3)	0.00(5)
2	std. gas-phase	93.6(5)	5.1(2)	5.1(3)	0.9(4)	0.41(8)	0.00(5)
3	std. w/o ICl	98.4	0.0	0.0	1.4	0.02	0.00
4	std. w/o NaN_3	97.6	0.0	0.0	1.1	0.39	0.97
5	std. w/o drying silica	98.8	<0.1	0.0	0.9	0.33	0.00
6	std. w/o drying $N_2(g)$	95.0	3.5	3.7	1.1	0.44	0.00
7	std. w/ 10% $O_2/Ar(g)$	94.3(4)	4.5(4)	4.5(4)	0.9(4)	0.32(8)	0.00(5)
8	std. w/ light	93.8(6)	4.9(2)	4.9(3)	0.9(4)	0.40(8)	0.00(5)
9	$I_2(g)$	98.2	0.0	0.0	1.5	0.30	0.00
10	hexane	90(2)	6.5(4)	6.0(4)	2(1)	0.6(3)	0.33(7)
11	acetonitrile	91(2)	5.1(4)	3.9(4)	3(1)	0.4(3)	0.6(1)

[a] Averaged value from three or more samples. Uncertainty of last significant figure, located in parentheses, is reported at 95% confidence interval with three or more independent data sets.

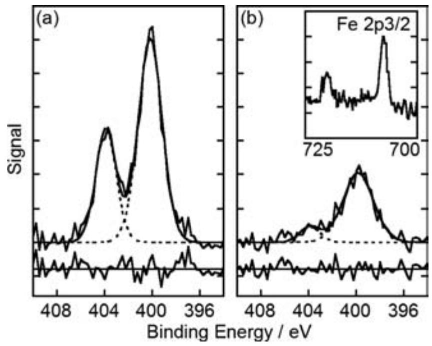

Figure 5. XPS spectra of N 1s region with fitted spectrum and residuals after subtraction of Shirley background for (a) gas-phase azide-modified surfaces and (b) ferrocene-modified surfaces with an insert of the Fe 2p region. Dotted lines are individual fitting components.

water by mass) led to surfaces with less than 0.1 atomic % nitrogen (Table 1, entry 5). Without drying the N_2 carrier gas, the $IN_3(g)$ concentration by UV/vis and the surface nitrogen concentration (Table 1, entry 6) are reduced. Replacing the N_2 carrier gas with dried 10% O_2/Ar decreases the surface nitrogen concentration to a small but statistically significant extent (Table 1, entry 7). Performing the gas-phase procedure under ambient lighting produced samples with similar elemental composition as in the dark (Table 1, entry 8). Because $I_2(g)$ was observed in the carrier gas stream, reduced glassy carbon was exposed independently to an $I_2(g)$ saturated nitrogen stream. This exposure to $I_2(g)$ resulted in iodine addition to the surface (Table 1, entry 9) with a concentration similar to that of the standard gas-phase procedure.

Solution Procedure for Azide Functionalization. Azide-modified glassy carbon surfaces were also prepared using previously reported solution methodologies.[21,22] Hydrogenated carbon surfaces react with IN_3 dissolved in hexane or acetonitrile, generated in situ from $NaN_3(s)$ and ICl(l). Hexane solutions produced surfaces with a higher azide surface concentration (6.0 atomic %), compared to the gas-phase procedure (5.1 atomic %), but contained some non-azide nitrogen species (0.5 atomic %) (Table 1, entry 10). Acetonitrile solutions produced the lowest surface azide concentration (3.9 atomic %) as well as significantly more non-azide nitrogen species (1.2 atomic %) (Table 1, entry 11). Measurable chlorine and higher oxygen concentrations were also observed on surfaces from solution preparations.

Surface Immobilization of Ethynylferrocene. Gas-phase azide-modified surfaces were treated overnight with 1.0 mM ethynylferrocene (**1a**), 1.0 mM tris(ethylacetyltriazolyl)-methylamine−Cu(II) nitrate, and 2.0 mM ascorbic acid in a $N_2(g)$-sparged 1:1 vol:vol mixture of dimethyl sulfoxide (DMSO) and H_2O to form a 1,2,3-triazole linkage between ferrocene and the surface (**2a**) through a CuAAC reaction. These surfaces were cleaned by sonication in DMSO. Fitting the XPS N 1s region separates the azide and non-azide nitrogen concentrations (Figure 5b). The stoichiometric 3:1 ratio of non-azide nitrogen to iron is consistent with formation of triazole linkage anticipated for **2a** (Table 2, entry 1). However, during the CuAAC reaction, loss of approximately half of the surface nitrogen occurred concurrently with triazole formation. Because all non-azide nitrogen is accounted for by triazole formation, this nitrogen loss is attributed to the loss of azide groups (N_3) from the surface. Azide loss was also observed during aqueous control experiments: in 1:1 DMSO:H_2O the azide concentration decreased from 5.1 ± 0.3 to 2.6 ± 0.5 atomic % in 2 h and was stable thereafter; no non-azide species were observed. In addition, the surface oxygen concentration increases from 1.1 ± 0.4 to 2.5 ± 0.7 atomic % over this time. In a separate control experiment, no changes in nitrogen or oxygen concentrations were observed for azide-modified surfaces under dry $N_2(g)$ overnight. Loss of approximately half the surface nitrogen also occurred under reducing conditions with 1.0 mM tris(ethylacetyltriazolyl)-

Table 2. XPS Atomic Concentrations for Ferrocene-Modified Surfaces (2a)

entry	azide prep.	C at. %[a]	N at. %[a]	azide at. %[a]	O at. %[a]	Fe at. %[a]	coverage[a,b] molecules/cm^2
1	gas-phase	94(1)	2.2(4)	1.0(3)	3.6(8)	0.37(4)	8(1) × 10^{13}
2	hexane	93(1)	2.5(5)	1.3(6)	3.8(6)	0.27(8)	6(1) × 10^{13}
3	acetonitrile	94(1)	1.8(2)	0.7(5)	4(1)	0.22(5)	3(1) × 10^{13}

[a] Averaged value from three or more samples. Uncertainty of last significant figure, located in parentheses, is reported at 95% confidence interval with three or more independent data sets. [b] Coverage determined by electrochemical methods.

methylamine−Cu(II) nitrate and 2.0 mM ascorbic acid in 1:1 DMSO:H_2O without an alkyne present. Similar to the previous control in DMSO:H_2O, this loss occurred over the initial 2 h and was stable thereafter. However, in contrast to the previous control, non-azide nitrogen species (1.2 atomic %) were observed along with unreacted azides (1.4 atomic %).

Scheme 1. Surface Immobilization on Carbon

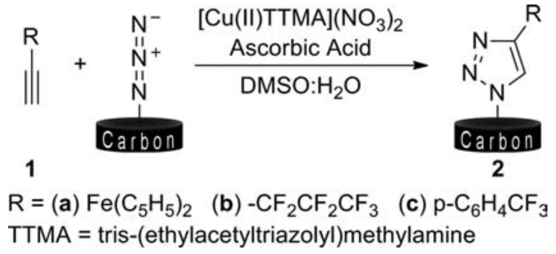

R = (**a**) $Fe(C_5H_5)_2$ (**b**) $-CF_2CF_2CF_3$ (**c**) p-$C_6H_4CF_3$
TTMA = tris-(ethylacetyltriazolyl)methylamine

Cyclic voltammetry of the ferrocene-modified carbon surfaces (**2a**) in 1 M $HClO_4$ displays a reversible peak at E^0 = 510 ± 10 mV vs NHE (Figure 6). The peak current varies linearly with scan rates from 0.5 to 10 V/s, consistent with surface-immobilized ferrocene. Electrochemical surface coverage of 8 ± 1 × 10^{13} ferrocene/cm^2 was obtained (Figure 6). The 170 ± 10 mV full-width at half-maximum of the cathodic peak, nearly twice the ideal Nernstian width, suggests heterogeneity or interaction among the ferrocene sites.[29] A standard electron-transfer rate of greater than 1000 s^{-1} is inferred from the 15 mV peak-to-peak splitting at a scan rate of 10 V/s.[30]

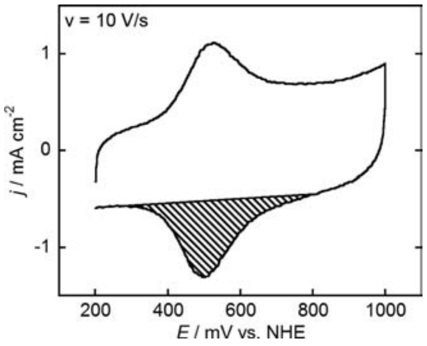

Figure 6. Cyclic voltammetry for gas-phase ferrocene-modified surface. Integration shown by shaded region.

Coupling of ethynylferrocene (**1a**) onto azide-modified surfaces prepared from IN_3 in solution led to statistically significantly lower ferrocene coverage as determined by both XPS and electrochemical measurements (Table 2, entries 2 and 3).[31] This is counterintuitive given the higher initial surface azide concentration from IN_3 in hexane solutions and is suggestive that gas-phase azide-modified surfaces have a greater propensity toward triazole formation.

Stability of the Immobilized Species. Under normal laboratory handling conditions, no nitrogen or iron loss was observed for ferrocene-modified surfaces (**2a**). To investigate the stability of immobilized species under harsher conditions, two fluorinated species, heptafluoropent-1-yne (**1b**) and 4-ethynyl-α,α,α-trifluorotoluene (**1c**), were immobilized on gas-phase azide-modified surfaces in a manner similar to that for ethynylferrocene (**1a**). These species are expected to be more robust than ferrocene while providing a high sensitivity XPS fluorine tag. The F 1s peak at 688 eV confirms immobilization of these species with fluorine concentrations of 2.4 ± 0.3 atomic % for heptafluoropropyl-modified surfaces (**2b**) and 0.9 ± 0.1 atomic % for trifluorotoluene-modified surfaces (**2c**) relative to all other surface atoms. As observed with ferrocene-modified surfaces (**2a**), nitrogen was lost during the CuAAC reactions for **2b** and **2c**. Non-azide nitrogen concentrations of 1.2 ± 0.2 atomic % and 0.9 ± 0.2 atomic % for **2b** and **2c** surfaces, respectively, are as expected from measured surface fluorine and primarily attributed to triazole formation.

The fluorine, azide nitrogen, and non-azide nitrogen surface concentrations in both 1 M $HClO_4$ and 1 M NaOH at 100 °C over a 12 h period were monitored by XPS. No perceivable change in non-azide nitrogen occurs for heptafluoropropyl-modified surfaces (**2b**) under acidic or basic conditions. However, fluorine and azide nitrogen are reduced (Figure 7a,b). Retention of fluorine is substantially greater under acidic than under basic conditions. Similar stability of surface species is observed for trifluorotoluene-modified surfaces (**2c**) where non-azide nitrogen is conserved but fluorine and azides are lost (Figure 7c,d). **2c** surfaces show a greater percent loss of fluorine than **2b** surfaces but no differentiation of fluorine stability under acidic or basic conditions.

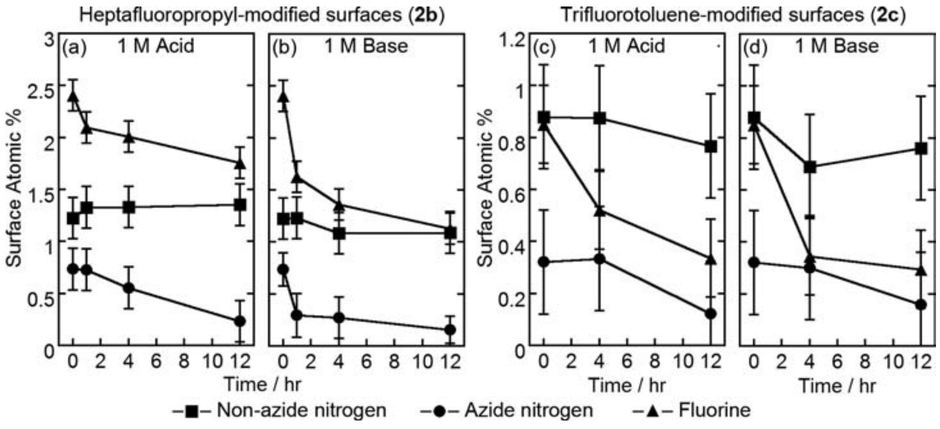

Figure 7. Stability of heptafluoropropyl-modified (**2b**) and trifluorotoluene-modified surfaces (**2c**) in both 1 M $HClO_4$ and 1 M NaOH at 100 °C measured by XPS. Error bars at 95% confidence interval.

DISCUSSION

Azide functionalization using IN_3 has been studied extensively in solution,[32,33] but its gas-phase reactivity has not previously been demonstrated. This may partially be due to the explosive dangers from the literature-reported preparation of gaseous IN_3 using $AgN_3(s)$, a very reactive azide reagent.[34,35] In contrast, contemporary solution methodologies pioneered by Hassner[36] use the in situ preparation of IN_3 from ICl(l) and the much more stable azide reagent, $NaN_3(s)$. The work here reports a convenient procedure for the preparation of gaseous $IN_3(g)$ by flowing ICl vapors over a column of $NaN_3(s)$ dispersed on silica. This procedure mitigates explosive risks by (i) using the more stable $NaN_3(s)$ reagent, (ii) minimizing the amount of $IN_3(g)$ prepared, (iii) limiting the rate of formation of $IN_3(g)$ by capitalizing on the low vapor pressure and rate of delivery of ICl(l) at room temperature, and (iv) diluting the prepared $IN_3(g)$ in a carrier gas stream. With these precautions in place, $IN_3(g)$ was prepared safely and used in the gas-phase azide functionalization of carbon surfaces.

Gas-phase reactivity of $IN_3(g)$ is inferred to proceed through a radical pathway by analogy to its solution reactivity, which favors radical pathways in low dielectric environments.[36] Reported radical reactivity of IN_3 in solution includes radical addition to olefins[36] and radical substitution of benzylic hydrogens.[37] Radical substitution reactivity would account for greater incorporation of azide than iodine, as is observed for azide-modified carbon in this study. In addition, much of the observed surface iodine concentration may be from the reaction of the I_2 byproduct with the reduced surface, as seen from the $I_2(g)$ control experiment (Table 1, entry 9).

The high selectivity and reproducibility of the gas-phase azide functionalization of glassy carbon, which produces surfaces containing azides as the sole nitrogen species, may stem from the ease with which the reaction environment can be controlled to reduce undesired side reactions. Decomposition of $IN_3(g)$ by water[35] is found to be detrimental to obtaining reproducibly functionalized surfaces. Thoroughly drying the N_2 carrier gas and the column of $NaN_3(s)$ dispersed on silica is essential. Additionally, protection of the hydrogenated carbon surfaces from atmospheric oxygenation[2] before azide functionalization is important. Gas-phase azide-modified surfaces have lower measurable oxygen concentrations than either solution azide-modified surfaces or hydrogenated surfaces after atmospheric exposure, suggesting that surface sites susceptible to oxygenation are instead blocked by azide functionalization. Because azide functionalization is observed to be at most slightly sensitive to dioxygen when dried 10% O_2/Ar is used as the carrier gas, it can be inferred that exclusion of water, not $O_2(g)$, is necessary to prevent surface oxygenation prior to azide functionalization. Another valuable aspect of this gas-phase procedure is the complete reaction of ICl as it moves through the column of $NaN_3(s)$, which prevents subsequent competition of ICl with IN_3 for sites on the hydrogenated carbon surface.

One use of azide-modified surfaces is as an effective handle for further surface functionalization by coupling to a variety of terminal alkyne species under the mild CuAAC reaction. Ferrocene-modified surfaces (**2a**) had coverages of $8 \pm 1 \times 10^{13}$ ferrocene/cm^2, approximately a third of a monolayer for densely packed ferrocene.[38] Similar coverage was achieved for heptafluoropropyl-modified (**2b**) and trifluorotoluene-modified (**2c**) surfaces as determined by XPS. An initial azide coverage before the CuAAC reaction of $3-4 \times 10^{14}$ azides cm^{-2} is extrapolated from the electrochemical coverage and XPS concentrations of ferrocene-modified surfaces. This azide coverage corresponds to a quarter of a densely packed monolayer on the zigzag edge of graphite. In actuality, because of the surface roughness, this is an overestimate and less than a quarter of a monolayer is actually azide functionalized.

Quantitative XPS analysis and modeling allows for the fate of surface azides to be followed through chemical transformations. During the CuAAC reaction and DMSO:H_2O control, azide loss was observed. This loss is postulated to occur by hydrolysis of the azide group from the surface because no evidence for other loss mechanisms, such as $N_2(g)$ loss upon azide reduction that should leave non-azide nitrogen on the surface, was observed. Hydrolysis of the azide group is also consistent with the measured increase in the surface oxygen concentration. The fact that approximately half of the surface azides of gas-phase modified surfaces are lost under aqueous conditions, while the remainder is stable, demonstrates a heterogeneous azide population. The origin of this azide heterogeneity is presumably a reflection of the underlying heterogeneity of the glassy carbon surface.

Azide reduction is inferred to occur under Cu(I) conditions without an alkyne present because nitrogen loss is accompanied by an increase in non-azide nitrogen species. These observations are consistent with the reduction of azide to an amine and loss of N_2, which is known to occur for various azides using a Cu(I) reductant.[39] As the entirety of nitrogen loss under these Cu(I) conditions can be accounted for by the N_2 loss upon azide reduction, reduction must occur faster than hydrolysis. The apparent lack of this reduction reaction during the CuAAC reaction suggests that interactions between the Cu(I) complex and an alkyne species disfavor the reductive pathway.

The triazole linker is stable toward hydrolytic cleavage in both 1 M acid and 1 M base for at least 12 h at 100 °C because no change was observed in non-azide nitrogen by XPS. However, under these harsh conditions, fluorine loss was observed for **2b** and **2c** surfaces. Fluorine loss is proposed to occur through hydrolysis of the CF_2 group alpha to the triazole; C−F bonds alpha to aromatic systems are known to undergo hydrolysis under strongly acidic and basic conditions.[40] C−F bond hydrolysis is observed to extend along the aliphatic CF_2 chains of the **2b** surfaces, consistent with literature precedent.[40]

CONCLUSIONS

In summary, the use of gaseous IN_3 under a controlled environment allows for the simple, scalable, reproducible, and chemically specific azide functionalization of carbon. The $IN_3(g)$ reagent can be safely prepared in-line from commercially available chemicals for immediate use in this gas-phase procedure. The controlled nature of this procedure reduces undesirable side reactions to produce azide-modified surfaces that contain no other nitrogen species. These azide-modified surfaces provide a handle for further functionalization by the coupling with terminal alkynes in a CuAAC reaction to create a hydrolytically robust triazole linker. The coverages of such immobilized species are improved relative to previous azide functionalization methods.

This procedure has been expanded beyond glassy carbon for the azide functionalization of other carbon materials, including several carbon black powders. These azide-modified materials are versatile substrates that are being modified for the rational design of functional materials, including the development of electrocatalytic surfaces.

■ EXPERIMENTAL SECTION

General Remarks. All chemicals were used as received unless otherwise stated. Hexane, acetonitrile (HPLC grade), dimethyl sulfoxide (BioReagents), ethanol (200 proof), ethynylferrocene, sodium hydroxide, perchloric acid, and iodine monochloride were obtained from Fisher Scientific. Copper(II) nitrate was obtained from Strem Chemicals, sodium azide from TCI America, L-(+)-ascorbic acid from J. T. Baker, 3,3,4,4,5,5,5-heptafluoropentyne from SynQuest, 4-ethynyl-*α*,*α*,*α*-trifluorotoluene from Sigma-Aldrich, and silia-P flash silica gel from Silicycle. All water used was deionized. Tris(ethylacetyltriazolyl)methylamine (TTMA) was prepared by a literature procedure.[41−43] All gases were obtained from Praxair. N_2 and 10% O_2/Ar were dried by passing over a drierite/5 Å molecular sieves column. Sigradur G glassy carbon disks with a 0.195 cm^2 geometric surface area were obtained from HTW Hochtemperatur-Werkstoffe GmbH. Wet/dry silicon carbide sandpaper 600 and 3000 grit were obtained from Partsmaster and USA1 Abrasives, respectively. The furnace tube is made of fused silica.

Analytical Instrumentation. X-ray photoelectron spectroscopy (XPS) was carried out on a Physical Electronics PHI 5000 Versaprobe spectrometer with Al K*α* radiation (1486 eV) at an angle of 45°. The CasaXPS software package was used for analysis and fitting of the spectra. Elemental composition was determined by the integration of all chemical species detected by XPS using the parameters for the sensitivity factors and starting/ending points with an averaging width of ±2.5 eV for the Shirley baseline in Table 3.

Table 3. XPS Sensitivity and Fitting Parameters

region	sensitivity	start/eV	end/eV
C 1s	0.314	297	279
N 1s	0.499	410	394
O 1s	0.733	538	525
I 3d5/2	6.302	625.6	613.6
Cl 2p	0.954	206	193
Fe 2p3/2	1.964	713	703
F 1s	1.000	693	683

Electrochemical measurements were recorded on a CV50W with a Pt counter electrode and an Ag/AgCl/KCl(sat) reference electrode. A Teflon cell with a face seal having an area of 0.1237 cm^2 was used to analyze the glassy carbon disks. The CV50W software package was used to record data. The reference was calibrated against both an Accumet Glass Body Ag/AgCl/4.0 M KCl(aq) electrode and an Accumet Glass Body saturated calomel electrode (SCE). All reported values are referenced to the normal hydrogen electrode (NHE). The aqueous electrolyte solution used for all electrochemical measurements was 1 M $HClO_4$.

Preparation of Glassy Carbon. Prior to each use, the carbon surfaces were prepared by sanding with 600 grit sandpaper for 30 s followed by polishing with 3000 grit sandpaper until surfaces appeared unmarred, approximately 90−120 s. Disks were cleaned by rinsing with water followed by sonication in water for 30 s to remove loose particles and dried in a stream of N_2(g).

Preparation of NaN_3(s) Dispersed on Silica. A 3.0 g amount of NaN_3(s) was dissolved in 100 mL of 60% EtOH:H_2O solution. A 9.25 g amount of silica was added (5 mmol NaN_3/g silica) and evaporated to a free-flowing powder under vacuum at 40 °C. The resultant NaN_3(s) dispersed on silica was further dried at 120 °C under vacuum overnight, losing an additional 5% weight.

Standard Gas-Phase Azide Functionalization Procedure. Warning: Azides are explosive in nature and proper precautionary steps should be undertaken. This gas-phase procedure was designed to mitigate the risks involved with the preparation and use of azide reagents. Care should be taken that the furnace is plumbed in stainless steel so that explosive metal azides do not build up as may occur in copper or lead plumbing.[44]

The polished glassy carbon disks were placed into a furnace and purged with forming gas (5% H_2 /N_2) at 2 L per minute (LPM) for 5 min. Under a flow of 2 LPM of forming gas, the furnace was heated to 1000 °C for 90 min to hydrogenate the carbon surfaces and then the furnace was cooled to room temperature over 1 h. NaN_3(s) dispersed on silica (5 mmol/g) was poured freely into the stainless steel lower chamber of a flow reactor, which was purged with dried N_2(g) for 10 min at 1 LPM. During this purging the flow reactor was heated to remove trace water. The reactor was placed in-line with the furnace at a N_2(g) flow rate of 1 LPM and 10 *μ*L of ICl(l) was injected into the upper chamber under positive N_2(g) pressure through an access port. ICl vapors were carried by N_2(g) and reacted with NaN_3(s) dispersed on silica to form IN_3(g). The gas stream containing IN_3(g) in turn reacts with the hydrogenate glassy carbon surfaces. Ten minutes after the injection of ICl(l), the furnace was purged at 2 LPM with N_2(g) for 1 min to remove any remaining IN_3(g) before removing the azide-modified glassy carbon. The functionalized glassy carbon was analyzed or used immediately.

Flow Reactor Design. The flow reactor consists of a 1/4 in. stainless steel upper and lower chamber connected by a 1/16 in. restriction (Figure 1). The lower chamber is 75 mm tall with a plug of glass wool supporting the NaN_3(s) dispersed on silica. The upper chamber contains a small bed of glass wool to absorb ICl(l) and is connected directly to a capped Swagelok t-joint to allow injection of ICl(l) under positive pressure.

N 1s Peak Fitting. The N 1s region was fit with two components. A higher energy component fixed at 403.9 eV with a full width at half-maximum of 2.0 eV and an unconstrained component around 400 eV. The parameters for the higher energy component were determined by fitting gas-phase azide-modified surfaces with a constrained two- or three-peak model with fixed areas to represent the distinct nitrogens of an azide.

Using the integrated area of the higher energy component (N^{+}_{area}) and the total integrated nitrogen area (N_{area}), the surface atomic concentration of azide can be calculated by:

$$\text{azide at. \%} = \frac{3 \times N^{+}_{\text{area}}}{N_{\text{area}}} \times \text{N at. \%}$$

The uncertainty in peak fitting was determined using Monte Carlo simulations in CasaXPS and is reported at the 95% confidence level. The uncertainty in the surface atomic concentration of azide is then given by the formula:

$$\sigma_{\text{azide at. \%}} = \frac{3 \times \sigma_{N^{+}_{\text{area}}}}{N_{\text{area}}} \times \text{N at. \%}$$

Solution Azide Functionalization Procedure. The polished carbon disks were placed into a furnace and purged with forming gas (5% H_2 /N_2) at 2 LPM for 5 min. Under a flow of 2 LPM of forming gas, the furnace was heated to 1000 °C for 90 min to hydrogenate the carbon surfaces and then the furnace was cooled to room temperature over 1 h. Preparation of IN_3 solutions was adapted from literature procedures.[21,22] A 10 *μ*L amount of ICl(l) was added to 0.1 g of NaN_3 in 10 mL of hexanes or dry acetonitrile. Significant solid, unreacted NaN_3 and NaCl product, were left undissolved at the bottom of the vial. These solutions were used immediately. Hydrogenated glassy carbon disks were placed into the solution for 1 h before being removed and rinsed with methanol.

Ferrocene-Modified (2a), Heptafluoropropyl-Modified (2b), and Trifluorotoluene-Modified (2c) Surfaces. An appropriate mass of the terminal-alkyne (**1a**−**c**) was dissolved in 5 mL of DMSO to produce a 2 mM stock solution. Five milliliters of a 2.0 mM tris(ethylacetyltriazolyl)methylamine−Cu(II) nitrate aqueous solution, prepared in a 1:1 molar ratio of tris(ethylacetyltriazolyl)methylamine and Cu(II) nitrate, was added to the DMSO solution. The 1:1 DMSO:H_2O solution was sparged with N_2(g) for 10 min. A 100 *μ*L amount of a 200 mM aqueous ascorbic acid solution was added to the DMSO:H_2O solution. Azide-modified glassy carbon was immersed in this solution for 14 h at room temperature before being cleaned by sonication for 10 min in DMSO followed by rinsing with water and drying in a stream of $N_2(g)$.

Stability of Surface Species. Heptafluoropropyl-modified (**2b**) and trifluorotoluene-modified (**2c**) surfaces were placed in both 1 M $HClO_4$ and 1 M NaOH for 0 to 12 h at 100 °C. At set time points, disks were removed and rinsed with water before being analyzed by XPS.

AUTHOR INFORMATION

Corresponding Author

chidsey@stanford.edu

Notes

The authors declare no competing financial interest.

ACKNOWLEDGMENTS

This work was supported by the US Department of Energy, Office of Basic Energy Sciences, as part of the Center for Electrocatalysis, Transport Phenomena and Materials for Innovative Energy Storage (CETM) Energy Frontier Research Center (EFRC) project number DE-SC00001055.

REFERENCES

(1) Liang, C.; Li, Z.; Dai, S. *Angew. Chem., Int. Ed.* **2008**, *47*, 3696−3717.

(2) McCreery, R. L. *Chem Rev* **2008**, *108*, 2646−2687.

(3) Yang, W.; Auciello, O.; Butler, J. E.; Cai, W.; Carlisle, J. A.; Gerbi, J. E.; Gruen, D. M.; Knickerbocker, T.; Lasseter, T. L.; Russell, J. N.; Smith, L. M.; Hamers, R. J. *Nat. Mater.* **2002**, *1*, 253−257.

(4) Lasseter, T. L.; Clare, B. H.; Abbott, N. L.; Hamers, R. J. *J. Am. Chem. Soc.* **2004**, *126*, 10220−10221.

(5) Downard, A. J. *Electroanalysis* **2000**, *12*, 1085−1096.

(6) Barriere, F.; Downard, A. J. *J. Solid State Electrochem.* **2008**, *12*, 1231−1244.

(7) Pinson, J.; Podvorica, F. *Chem. Soc. Rev.* **2005**, *34*, 429−439.

(8) Nielsen, L. T.; Vase, K. H.; Dong, M.; Besenbacher, F.; Pedersen, S. U.; Daasbjerg, K. *J. Am. Chem. Soc.* **2007**, *129*, 1888−1889.

(9) Combellas, C.; Jiang, D. E.; Kanoufi, F.; Pinson, J.; Podvorica, F. *Langmuir* **2009**, *25*, 286−293.

(10) Leroux, Y. R.; Fei, H.; Noel, J. M.; Roux, C.; Hapiot, P. *J. Am. Chem. Soc.* **2010**, *132*, 14039−14041.

(11) Kongsfelt, M.; Vinther, J.; Malmos, K.; Ceccato, M.; Torbensen, K.; Knudsen, C. S.; Gothelf, K. V.; Pedersen, S. U.; Daasbjerg, K. *J. Am. Chem. Soc.* **2011**, *133*, 3788−3791.

(12) Downard, A. J.; Garrett, D. J.; Tan, E. S. *Langmuir* **2006**, *22*, 10739−10746.

(13) Ssenyange, S.; Anariba, F.; Bocian, D. F.; McCreery, R. L. *Langmuir* **2005**, *21*, 11105−11112.

(14) Sun, B.; Colavita, P. E.; Kim, H.; Lockett, M.; Marcus, M. S.; Smith, L. M.; Hamers, R. J. *Langmuir* **2006**, *22*, 9598−9605.

(15) Yu, S. S.; Downard, A. J. *Langmuir* **2007**, *23*, 4662−4668.

(16) Tornoe, C. W.; Christensen, C.; Meldal, M. *J. Org. Chem.* **2002**, *67*, 3057−3064.

(17) Rostovtsev, V. V.; Green, L. G.; Fokin, V. V.; Sharpless, K. B. *Angew. Chem., Int. Ed.* **2002**, *41*, 2596−2599.

(18) Kolb, H. C.; Finn, M. G.; Sharpless, K. B. *Angew. Chem., Int. Ed.* **2001**, *40*, 2004−2021.

(19) Evans, R. A. *Aust. J. Chem.* **2007**, *60*, 384−395.

(20) Iha, R. K.; Wooley, K. L.; Nystrom, A. M.; Burke, D. J.; Kade, M. J.; Hawker, C. J. *Chem. Rev.* **2009**, *109*, 5620−5686.

(21) McCrory, C. C. L.; Devadoss, A.; Ottenwaelder, X.; Lowe, R. D.; Stack, T. D. P.; Chidsey, C. E. D. *J. Am. Chem. Soc.* **2011**, *133*, 3696−3699.

(22) Devadoss, A.; Chidsey, C. E. D. *J. Am. Chem. Soc.* **2007**, *129*, 5370−5371.

(23) Schulz, A.; Tornieporth-Oetting, I. C.; Klapoetke, T. M. *Inorg. Chem.* **1995**, *34*, 4343−4346.

(24) Engelhardt, U.; Feuerhahn, M.; Minkwitz, R. *Z. Anorg. Allg. Chem.* **1978**, *440*, 210−216.

(25) Tellinghuisen, J. *J. Chem. Phys.* **1973**, *58*, 2821−2834.

(26) Variance in $IN_3(g)$ onset for the IR and UV/vis gas cells were seen and postulated to be dependent on laboratory temperature and $NaN_3(s)$ dispersed on silica column packing but was not further investigated.

(27) Collman, J. P.; Devaraj, N. K.; Eberspacher, T. P. A.; Chidsey, C. E. D. *Langmuir* **2006**, *22*, 2457−2464.

(28) Qu, Z.; Yan, N.; Liu, P.; Jia, J.; Yang, S. *J. Hazard. Mater.* **2010**, *183*, 132−137.

(29) Bard, A. J.; Faulkner, L. R. *Electrochemical Methods: Fundamentals and Applications*, 2nd ed.; John Wiley & Sons, Inc.: New York, 2001.

(30) Laviron, E. *J. Electroanal. Chem.* **1979**, *101*, 19−28.

(31) This lower ferrocene coverage is not due to differences in azide loss; azide concentrations of acetonitrile and hexane azide-modified surfaces decreased from 3.9 ± 0.4 to 3.7 ± 0.4 atomic % and 6.0 ± 0.4 to 4.1 ± 0.5 atomic % in DMSO:H_2O over 2 h, respectively, significantly less than for gas-phase azide-modified surfaces.

(32) Dehnicke, K. *Angew. Chem., Int. Ed.* **1979**, *18*, 507−514.

(33) Bräse, S.; Gil, C.; Knepper, K.; Zimmermann, V. *Angew. Chem., Int. Ed.* **2005**, *44*, 5188−5240.

(34) Hargittai, M.; Molnar, J.; Klapoetke, T. M.; Tornieporth-Oetting, I. C.; Kolonits, M.; Hargittai, I. *J. Phys. Chem.* **1994**, *98*, 10095−10097.

(35) Munz, H. *J. Mol. Struct.* **2004**, *695*, 189−202.

(36) Hassner, A. *Acc. Chem. Res.* **1971**, *4*, 9−16.

(37) Viuf, C.; Bols, M. *Angew. Chem., Int. Ed.* **2001**, *40*, 623−625.

(38) Chidsey, C. E. D.; Bertozzi, C. R.; Putvinski, T. M.; Mujsce, A. M. *J. Am. Chem. Soc.* **1990**, *112*, 4301−4306.

(39) Xia, Y.; Li, W.; Qu, F.; Fan, Z.; Liu, X.; Berro, C.; Rauzy, E.; Peng, L. *Org. Biomol. Chem.* **2007**, *5*, 1695−1701.

(40) Hudlicky, M. *Chemistry of Organic Fluorine Compounds: a Laboratory Manual with Comprehensive Literature Coverage*, 2nd ed.; Ellis Horwood: New York, 1992.

(41) Zhou, X.; Chang, Y.-C.; Oyama, T.; McGuire, M. J.; Brown, K. C. *J. Am. Chem. Soc.* **2004**, *126*, 15656−15657.

(42) Chan, T. R.; Hilgraf, R.; Sharpless, K. B.; Fokin, V. V. *Org. Lett.* **2004**, *6*, 2853−2855.

(43) Wang, Q.; Chan, T. R.; Hilgraf, R.; Fokin, V. V.; Sharpless, K. B.; Finn, M. G. *J. Am. Chem. Soc.* **2003**, *125*, 3192−3193.

(44) *CRC Handbook of Chemistry and Physics*, 92nd ed.; CRC Press: Boca Raton, FL, 2011/2012.